Mon. Not. R. Astron. Soc. **000**, 000–000 (0000) Printed 13 February 1998 (MN LaTeX style file v1.3)

The new Intermediate Polar RX J1238–38: a system below the period gap ?

David A. H. Buckley[1,3], Mark Cropper[2], Gavin Ramsay[2]
& Dayal T. Wickramasinghe[3]

[1] *South African Astronomical Observatory, PO Box 9, Observatory 7935, Cape Town, South Africa*
[2] *Mullard Space Science Laboratory, University College London, Holmbury St. Mary, Dorking, Surrey, RH5 6NT, UK*
[3] *The Astrophysical Theory Centre, School of Mathematical Sciences, The Australian National University, Canberra, ACT 0200, Australia*

Accepted. Received 1997 Feb 30; in original form 1995 April

ABSTRACT

We present optical observations of the recently discovered *ROSAT* source, RX J1238–38, which is a new member of the Intermediate Polar class of asynchronous magnetic cataclysmic variables. Optical photometry reveals two coherent periodicities at 1860 s and 2147 s respectively, with similar amplitudes of ∼8%. Infrared (*J*-band) intensity variations are detected only at the 1860 s period, at an amplitude of ∼15%. The initial hypothesis, that these two periods were the spin and synodic (i.e. beat) period respectively, appears not to be supported by the spectroscopic data. The emission lines vary on the longer photometric period, and radial velocity variations are detected at this, and a longer period at ∼5300 s, which we identify as the spin and orbital periods, respectively. The most likely explanation for the 1860 s period is that it is the first harmonic of the $\omega - \Omega$ sideband, leading to an improved determination of the orbital period as 5077 s (= 84 min). If this interpretation is correct, RX J1238–38 joins EX Hya as the only other Intermediate Polar below the 2−3 hour period gap, and with an orbital period close to the minimum for CVs with non-degenerate secondaries. The spin modulated emission line radial velocities and widths appear to be anti-correlated, with maximum width occuring at maximum blueshift. Such an anti-correlation is expected for aspect changes of accretion curtains. Polarimetric observations of RX J1238–38 were inconclusive, although we can put a limit of 0.4% on any variability on the circular polarization, and certainly there is no indication of variations at the photometric or spectroscopic periods.

Key words: Stars: accretion, accretion discs - stars: individual: RX J1238–38- stars: magnetic fields - X-rays: stars - novae, cataclysmic variables - white dwarfs - Xrays: stars

1 INTRODUCTION

The *ROSAT* soft X-ray and extreme UV surveys have been particularly successful in identifying new magnetic cataclysmic variables, especially the synchronised, stronger field, polars (AM Herculis systems). In recent times a number of new intermediate polars (IPs, or DQ Herculis systems) have also been identified from the *ROSAT* surveys (e.g. Mason et al. 1991, Buckley et al. 1995, Haberl & Motch 1995, Motch et al. 1996). Whereas most IPs are generally characterised by a single hard bremsstrahlung (kT $\gtrsim$10 keV) X-ray spectrum, many of the new *ROSAT* discoveries are also seen to exhibit an additional soft, blackbody-like, component (Haberl & Motch 1995). In this respect they resemble their relatives, the polars.

In this paper we report the discovery of the new *ROSAT* IP, RX J1238–38, discovered during the ROSAT All-Sky Survey. We first report on extensive high-speed and CCD photometric observations, which reveals two coherent periodicities, at 1860 s and 2147 s, with amplitudes of ∼8%. Next we report on optical and IR polarimetric observations, which fail to conclusively detect periodic polarization variations. Finally we present spectroscopic observations of RX J1238–38, which show that the line emission is pulsed at the longer photometric period of 2147 s. In addition, radial velocity variations are detected at this same period and at 5077 s, which we identify as the most likely spin and orbital periods.

We conclude with a discussion of the observed properties, and conclude that the system may be an example

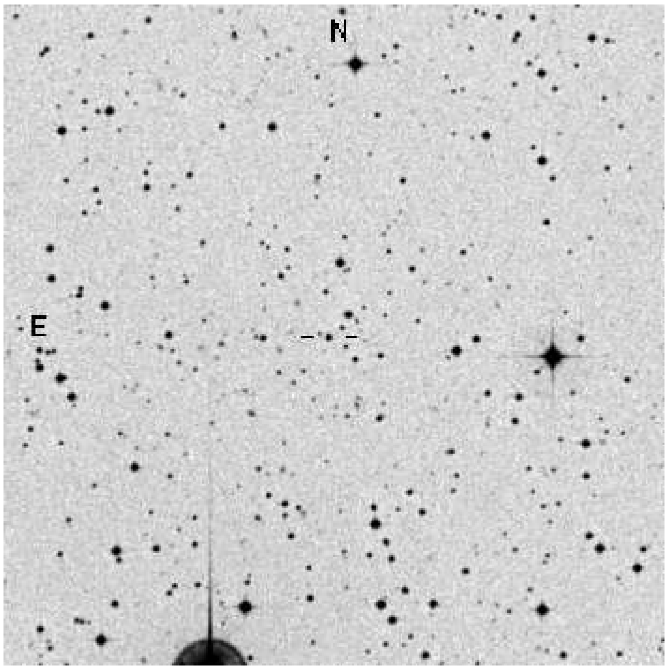

Figure 1. Finding chart (10 × 10 arcmin) for RX J1238–38. R.A. = $12^{H}38^{M}16.3^{S}$Dec = $-38°42'45.4''$ (errors $\pm 2''$)

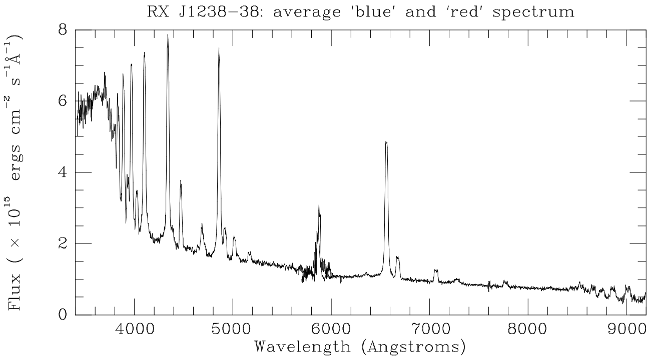

Figure 2. Mean combined spectrum of RX J1238–38.

of an IP which is possibly accreting through *both* proposed modes of accretion: directly from the stream penetrating to the magnetosphere, and via a partially truncated accretion disc.

2 THE ROSAT SOURCE RX J1238–38 AND ITS IDENTIFICATION

RX J1238–38 was observed for 319 sec during the *ROSAT* all-sky survey (Voges et al 1997). The total count rate was 0.52±0.04 ct s^{-1} (0.1-2.4keV and corrected for vignetting). The X-ray position is R.A. = $12^{H}38^{M}16.6^{S}$ Dec = $-38°42'43''$ (J2000), with an uncertainty of ±7 arcsec, which includes the systematic pointing errors.

Spectroscopy of a ∼16th magnitude star, at the source position, was undertaken using the ESO 3.6-m telescope. The spectrum (courtesy of M. Pierre) is typical of a CV, with intense Balmer emission, and lines of HeI and HeII. The strength of the HeII 4686 line, which is often taken as an indication that the system is magnetic, is much less than Hβ. For polars, the HeII line is often as strong or stronger than Hβ, whereas for IPs, the situation is less clear, since the ratio is seen to be quite variable (Szkody 1995). On the basis of the positional coincidence, and the properties of the CV, we conclude that it is firmly established as the optical counterpart of RX J1238–38. A finding chart of the new CV, taken from the Digital Sky Survey, is shown in Fig. 1, and the coordinates (J2000) of the CV are R.A. = $12^{H}38^{M}16.3^{S}$ Dec = $-38°42'45.4''$ (errors $\pm 2''$). In Fig.2 we display our mean spectrum derived from the spectroscopic observations reported in Section 3.4 (the 'red' and 'blue' spectra are both plotted).

To make a comparison of RX J1238–38 with *ROSAT* observations of other CVs which were observed in the all-sky survey (Verbunt et al 1997), we can make use of the two standard hardness ratios: HR1=0.77±0.05 (0.5:2.0keV–0.1:0.4keV)/(0.5:2.0keV+0.1:0.4keV) and HR2=0.27±0.08 (0.9:2.0keV–0.5:0.90keV)/(0.9:2.0keV+0.5:0.90keV).

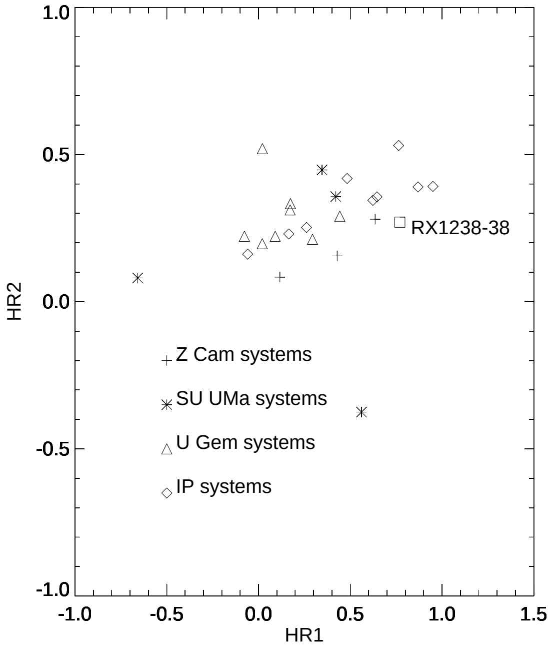

Figure 3. The *ROSAT* hardness ratios of various sub-classes of CVs (from Verbunt et al 1997) and RX J1238–38. They are defined in terms of fluxes in the following bands. HR1: (0.5:2.0 keV)–(0.1:0.4 keV)/(0.5:2.0 keV)+(0.1:0.4 keV) and HR2: (0.9:2.0 keV)–(0.5:0.9 keV)/(0.9:2.0 keV)+(0.5:0.9 keV).

Figure 3 shows those systems reported in Verbunt et al. (1997), which had non-zero counts in all of the above bands, in the HR1 verses HR2 plane. In addition, we have plotted the hardness ratios of three IPs discovered using *ROSAT* (RX J0028+59, RX J0153+74 and RX J1712–24: Haberl & Motch 1995) which were taken from the *ROSAT* all-sky survey archive (Voges et al 1997). RX J1238–38 falls in the same location in this diagram as a number of IPs, although it is close to some SU UMa, U Gem and Z Cam sub-classes of dwarf novae.

Table 1. Observing Log for RX J1238–38

DATE (day	month	year)	RUN	TELESCOPE	HJD START (-2440000)	LENGTH (h)	INT (s)	FILTER/ WAVELENGTH
High-speed photometry:								
30/31	Mar	95	S9807	SAAO 0.75 m	9807.320	8.15	5	wl
31/1	Mar/Apr	95	S9808	SAAO 0.75 m	9808.255	9.75	5	wl
1/2	Apr	95	S9809	SAAO 0.75 m	9809.273	9.29	5	wl
2/3	Apr	95	S9810	SAAO 0.75 m	9810.283	8.97	5	wl
3/4	Apr	95	S9811	SAAO 0.75 m	9811.249	4.25	5	wl
15/16	Feb	96	S0129	SAAO 0.75 m	10129.545	2.19	10	wl
16/17	Feb	96	S0130	SAAO 0.75 m	10130.500	3.22	10	wl
17/18	Feb	96	S0131	SAAO 0.75 m	10131.502	0.93	10	wl
18/19	Feb	96	S0132	SAAO 0.75 m	10132.489	3.42	10	wl
CCD photometry:								
26/27	Apr	95	C1	SAAO 1.9 m	9834.311	3.38	30	I
27/28	Apr	95	C2	SAAO 1.9 m	9835.239	2.68	30	BI
28/29	Apr	95	C3	SAAO 1.9 m	9836.264	6.17	30	BI
29/30	Apr	95	C4	SAAO 1.9 m	9837.245	3.63	30	BVRI
30/1	Apr/May	95	C5	SAAO 1.9-m	9838.251	3.29	30	BI
Polarimetry:								
16/17	Feb	96	P0130	SAAO 1.9 m	10130.550	1.68	100	OG570
17/18	Feb	96	P0131	SAAO 1.0 m	10131.500	0.84	100	OG570
18/19	Feb	96	P0132	SAAO 1.9 m	10132.411	4.85	100	OG570
15	Mar	96	U0157	UKIRT 3.5 m	10157.967	1.80	60	J
16	Mar	96	U0158	UKIRT 3.5 m	10158.963	1.82	60	J
17	Mar	96	U0159	UKIRT 3.5 m	10159.954	1.70	60	J
18	Mar	96	U0160	UKIRT 3.5 m	10160.956	1.80	60	J
19/20	Mar	96	P0162	SAAO 1.9 m	10162.330	3.12	100	wl
20/21	Mar	96	P0163	SAAO 1.9 m	10163.320	5.64	100	wl
24/25	Mar	96	P0167	SAAO 1.9 m	10167.488	3.57	100	OG570
Spectroscopy:								
19	Apr	96	SSO96	SSO 2.3 m	10194.885	3.48	100	3400−6000Å
19	Apr	96	SSO96	SSO 2.3 m	10194.885	3.48	100	6000−9100Å

3 OBSERVATIONS

3.1 Photoelectric photometry

White-light (i.e. un-filtered) high-speed photometry of RX J1238–38 was initially undertaken in 1995 March-April (see Table 1 for observing log), using the UCT Photometer on the SAAO 0.75-m telescope. Data were obtained on 5 consecutive nights, with 10 s integration times. Before a time series analysis was performed, the data were corrected for sky background and extinction (using empirical coefficients). A UBV measurement (in the symmetrical observing sequence VBUBV) of RX J1238–38 was obtained on 1995 April 1/2 (with the same instrumentation), which gave the following magnitude and colours: V = 16.12, B-V = −0.09 and U-B = −1.22. Further high-speed photometry was conducted during 1996 February 15−18, during a simultaneous polarimetry run (see below), using the same telescope but with the Radcliffe Peoples Photometer (RPP). Again, white-light observations were undertaken with an S20 photomultiplier.

In Fig. 4 we show the light curves for RX J1238–38 obtained from the twelve nights of high-speed photometry in 1995 February and 1996 February and March. The data have been normalised by the mean count rate on each night by first dividing the data by the mean, and then subtracting unity. The resulting light curves therefore represent the fractional change in the intensity. Variability typical of a CV is seen, with variations of up to ∼50%. To the trained eye, the light curves show possible periodic variations, and in Section 4 we investigate this in detail. The 1996 March data ('JD 10162–10167' in Fig. 4) are from the polarimetry observations, reported in section 3.3.

3.2 CCD photometry

CCD photometry of RX J1238–38 was carried out later in 1995 April (see Table 1) using the SAAO Tek8 CCD (512 × 512 × 24 μm pixels) on the 1.9-m telescope. On-chip 3 × 3 prebinning was used in order not to oversample the PSF, with the resulting scale being 0.52 arcseconds pixel^{-1}. Consecutive 30 s exposures in two or four of the BVR_CI_C filters were taken (e.g. B & I or B, V, R_C & I_C). Following the usual flat fielding corrections and bias subtraction, the individual cleaned frames were reduced using the *DoPHOT* package (Mateo & Schechter 1989) to derive both PSF fitted,

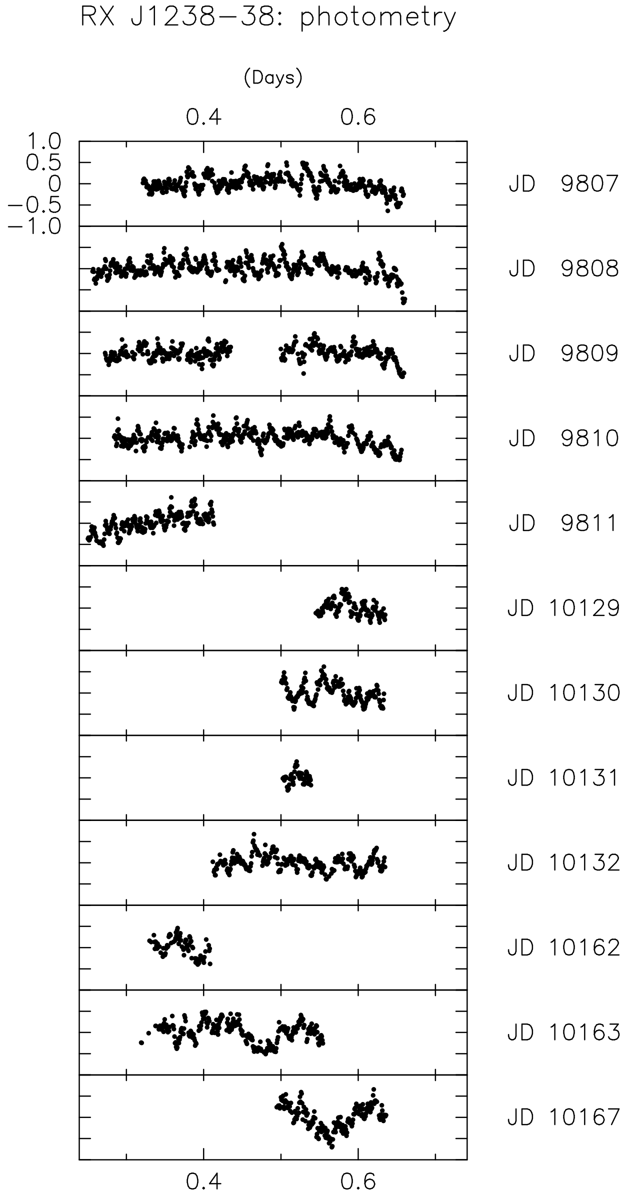

Figure 4. Normalized high-speed photometry light curves of RX J1238–38 . The ordinate represents the fractional variation from the mean light (±100%). Numbers on the right represent JD day numbers – 2440000 (see log).

and aperture, magnitudes. Observations of E-region standard stars (Menzies et al. 1990) were used to define the instrumental zero points, and to transform the instrumental magnitudes to the natural *BVRI* system. Fig. 5 shows a montage of the *B & I* CCD light curves of RX J1238–38. The less extensive *V & R* data set show essentially the same information, and are not shown.

3.3 Polarimetry

Photopolarimetry of RX J1238–38 was undertaken at the SAAO in 1996 February and March, using the UCT Polarimeter (Cropper 1985) on the 1.9 m telescope. The instrument uses two counter-rotating (at 10Hz) 1/4 and 1/2 superachromatic waveplates, which modulates the signal. Fourier series are then fitted to an accumulated counts buffer, and the Stokes parameters Q, U and V determined from the $4\theta, 6\theta$ and 8θ terms. This so-called "Stoke's mode" of operation allows for simultaneous determination of both linear and circular polarization. Typical integration times for the polarizations were 100 s, while simultaneous intensity measurements were obtained at the higher time resolution of 10 s. These were included in the photometric analysis (Section 4). The observations were obtained either in the photomultiplier-defined (S20) "white-light", or through a broad red OG570 filter, which has a blue cut-on at ∼5700Åand a cut-off defined by the red sensitivity limit of the S20 photomultiplier.

Imaging IR polarimetry of RX J1238–38 was obtained, on UKIRT, using IRCAM3+IRPOL2 from 1996 March 15−18. IRCAM3 is a cooled 1-5μm camera with a 256 × 256 InSb array and IRPOL2 uses a warm half waveplate and focal plane mask with a cold Wollaston prism to produce o- and e- ray images on the array. The Q and U Stokes parameters are obtained by rotating the waveplate through steps of 22.5 degrees. The images were chopped between two locations on the array using the secondary mirror after a sequence of 4 waveplate rotations was completed. The images were built into a time sequence, and flatfielded using the two flats created from the interleaved frames in which the image had been chopped to the other location on the array. The centroids of each image were located and aperture photometry used to extract the flux from each image to create the light and polarisation curves. Software apertures of 5 arcsec were used in conditions in which the seeing was ∼ 1.2 arcsec. This was the best compromise between introducing systematic effects and minimising the background in the aperture. Annuli of 5 arcsec (inner) to 10 (outer) arcsec diameter were used for background subtraction. Linear and zero polarisation standards (Serkowski 1974 and Whittet et al. 1992) were used to calibrate the instrument: in the J-band we measured the efficiency to be 0.77 ± 0.03 and the Stokes Q and U instrumental polarisations were measured as 0.46 percent and 0.17 percent. These corrections and the position angle zero point were applied to the data.

3.4 Spectroscopy

Time resolved spectroscopy of RX J1238–38 was undertaken on 1996 April 19 using the Double Beam Spectrograph on the Australian National University 2.3 m telescope at Siding Springs Observatory (SSO). The 'blue' and 'red' arms of the spectrograph covered the range 3400−6000Å and 5800−9100Å, respectively, at a reciprocal dispersion of 2Å pixel^{-1}. Observations were obtained with the slit orientated to the parallactic angle, to avoid atmospheric dispersion effects. Comparison arc spectra were taken every ∼2000 s, and bias frames and flat fields taken at the beginning and end of the observations. The IRAF⋆ spectroscopic tasks **ccdproc**, **onedspec** and **twodspec** were used to produce wavelength and flux calibrated spectra of RX J1238–38. The mean combined blue-red spectrum of RX J1238–38 is shown

⋆ IRAF is distributed by NOAO, which operated by AURA, Inc., under contract to the NSF.

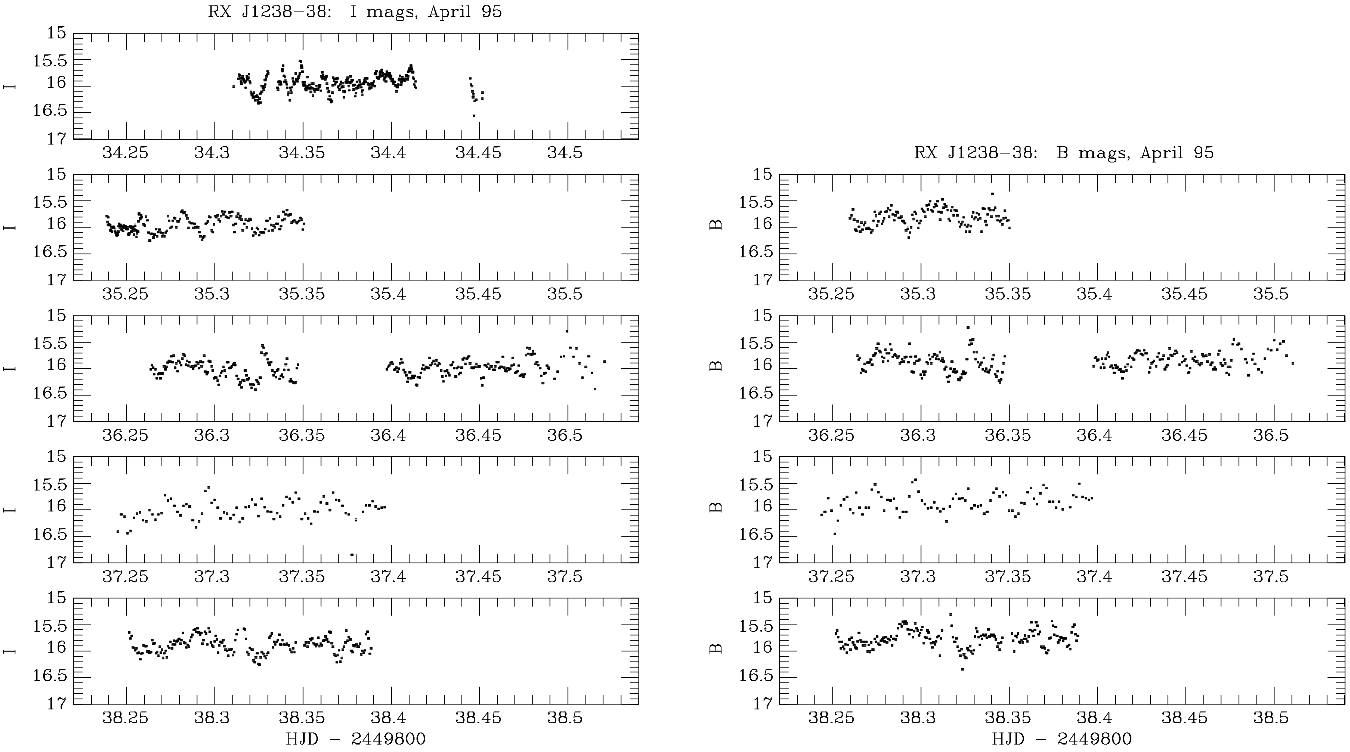

Figure 5. *I*- and *B*-band CCD light curves of RX J1238–38, taken simultaneously in 1995 April.

in Fig. 2. It is clear that the emission lines are very broad, and multi-component in nature. The typical FWHM of the lines is ∼1600 km s^{-1}, although a much broader component is also seen, with a FWZI of up to 5000−6000 km s^{-1}. Such lines are typical of IPs, and in Section 6 we investigate the line variability in more detail.

No secondary star features (TiO bands, NaI absorption) were seen in our red spectra of RX J1238–38, precluding a determination of the secondary star's radial spectral typing or velocity curve.

4 PHOTOMETRIC PERIOD ANALYSIS

4.1 Optical photometry

The entire 1995 high-speed photometric time series were subjected to a period analysis using a standard discrete Fourier transform (DFT) code (Deeming 1975, Kurtz 1985). In the top two panels of Fig. 6, we show the DFT amplitude spectra, which shows strong evidence for multi-periodic variability, namely the presence of two strong peaks at ∼2146.6 and 1859.5 s, and their 1 cycle d^{-1} aliases. We performed a least-squares sine fit of the longer, marginally stronger, period. This fit was then used to pre-whiten the data, and the amplitude spectrum recalculated (second panel of Fig. 6). The fact that the 1860 s period is unaffected in this prewhitening procedure confirms the reality of the two distinct periods, rather than them being a artifact of the data sampling. Indeed the window function confirms this, showing the typical aliased single frequency. Although it is possible that nearby aliases are the true periods, the symmetry of the frequency peaks, and their relative amplitudes, argue against this. Note too that the periodograms in Fig. 6 are plotted in amplitude, rather than power, so the 2147 s and 1860 s peaks would thus appear even more significant in power spectra.

The only other significant peaks are those at low frequencies (at ∼0.035 and 0.057 mHz, and 1 cycle d^{-1} aliases). Such low frequencies are often associated with long-term trends introduced by extinction, although we have been careful in attempting to remove such variations during the data reduction. We investigated higher frequencies, up to the Nyquist limit, but found nothing significant, including the presence of harmonics of the previously identified frequencies.

The remaining datasets (1995 CCD photometry and 1996 high-speed photometry) were analysed in an identical manner. Amplitude spectra from these runs are also included in Fig. 6. Both data sets confirmed the presence of the two periods at 2147 and 1860 s, although significant differences were also seen. In particular the 1996 data showed evidence for lower frequency variability, in the region 0.06–0.2 mHz (periods ∼1.4–4.7 h).

Of note in the CCD periodograms is the apparent wavelength dependency of the amplitudes of the two main periods, as seen in the *B*- and *I*-band CCD light curves. Whereas in the *B* light curve the longer period (2147 s) dominates, the reverse was the case in the case of the *I*-band, where the 1860 s period is relatively more dominant. The 2147 s amplitude is also somewhat higher in *B*.

We have determined the mean phase binned light curve at the 2147 and 1860 s period, by first pre-whitening the other period, and then phase binning the data. The results for the 1995 high-speed photometry are presented in

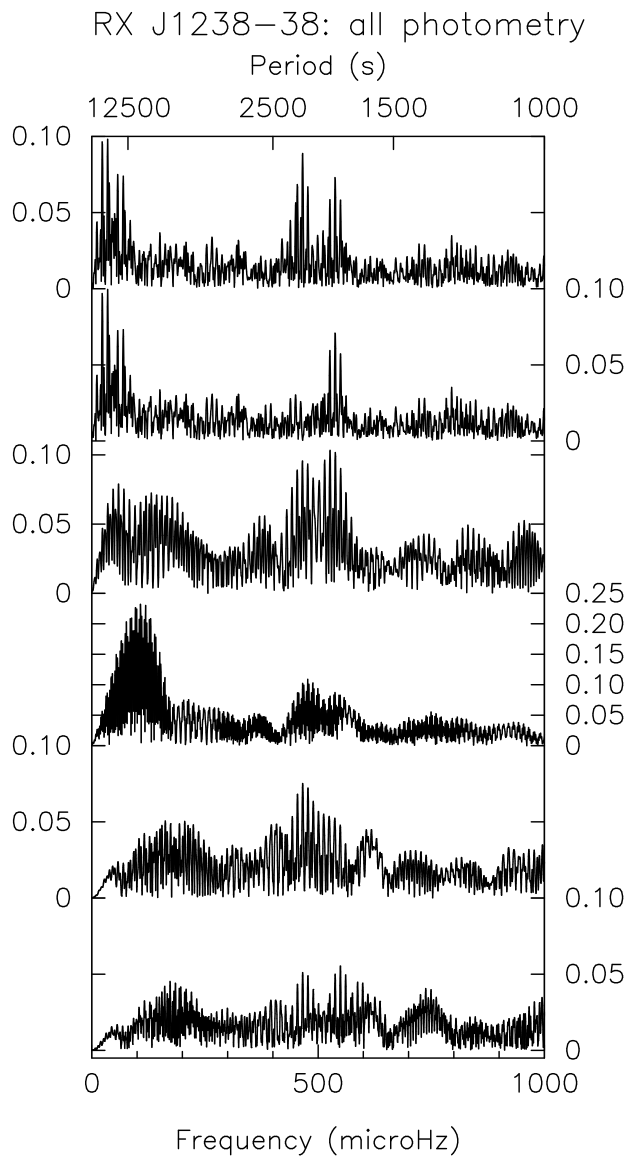

Figure 6. DFT amplitude spectra of RX J1238–38 photometry (see text). Graphs correspond, from top (1) to bottom (6), to: March/April 95 high-speed photometry, before (1) and after (2) pre-whitening of the 2147 s period, 1996 high-speed photometry (3 = Feb; 4 = March), CCD photometry (5 = B-band; 6 = I-band). The ordinate represents the amplitude as a fraction of the mean (i.e. 0 to 10%)

Table 2. Amplitudes and phases of the sinusoids fitted to the two dominant periods.

Period (s)	*Frequency* (Hz)	*Amplitude* (%)	T_{MAX} (HJD–2440000)
2146.59	4.6585×10^{-4}	8.9 ± 0.3	9807.308(7)
1859.50	5.3778×10^{-4}	7.2 ± 0.3	9807.319(5)

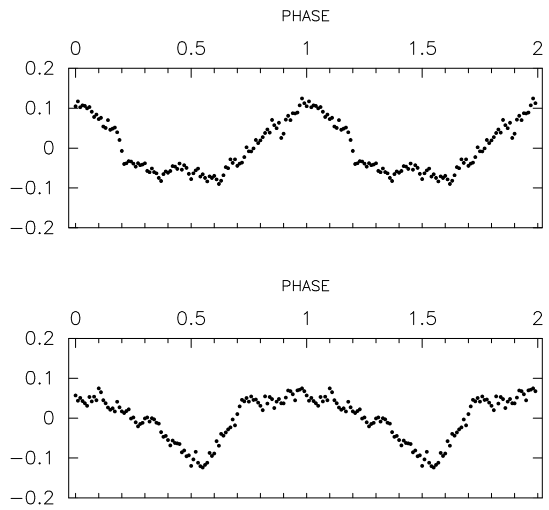

Figure 7. Optical light curve of RX J1238–38 folded on the 2147 s (top) and 1860 s (bottom) photometric periods. The ordinate is fractional intensity variation from mean light (i.e. a range of ±20% variation).

Fig 7. The amplitudes and phases maximum light for the two periodic signals are given in Table 2. Both signals are clearly non-sinusoidal, with the 2147 s period showing a more sharply peaked maximum and flat minimum, and *vice versa* for the 1860 s period.

Periodic variability at ∼1000 s is a typical characteristic of an Intermediate Polar (e.g. Patterson 1994), and is usually associated with either the spin period of the white dwarf, or the synodic period produced from interference of the spin and orbital frequencies (i.e. a beat period). The fact that we see the same periodicities in all three observing runs, separated by $\gtrsim$1 year, argues in favour of a coherent period, as in an IP. Optical and X-ray photometry of IPs often reveal rich frequency spectra, with periods attributed to the spin (ω), orbital (Ω) and orbital sideband ($\omega-2\Omega, \omega-\Omega, \omega+\Omega$ and $\omega+2\Omega$) frequencies (Warner 1986). Normally either the spin frequency, ω, or the first orbital sideband (the synodic, or beat, frequency), $\omega-\Omega$, dominates the optical variability in an IP (see Warner 1995). Only in one system, AO Psc, have nearly equal amplitudes been seen in *both* spin and synodic periods (van der Woerd, de Kool & van Paradijs 1984). However, it is more usual that the synodic period dominates (Warner, O'Donoghue & Fairall 1981). For RX J1238–38 we see that both photometric periods have nearly equal amplitudes in all high-speed data, with the longer period (2147 s) marginally stronger than the shorter (1860 s) during 1995, and *vice versa* in 1996.

If we interpret the 1860 s period as arising from the spin modulation, and identify the 2147 s period as the first orbital sideband ($\omega-\Omega$), then we logically arrive at the conclusion that the orbital period has to be the difference in these frequencies, namely 3.86 hours (0.072 mHz). Although some low frequencies are seen, on occasions, in the optical photometry, this particular period is not detected. In Section 6 we investigate if this hypothesis is further supported by the spectroscopic observations.

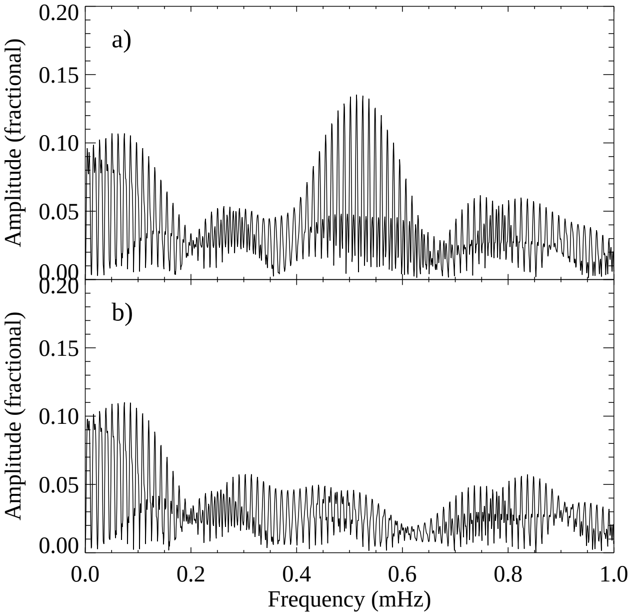

Figure 8. DFT amplitude spectrum for the *J*-band light curve of RX J1238–38 , before (top) and after pre-whitening (bottom) the 1860 s period.

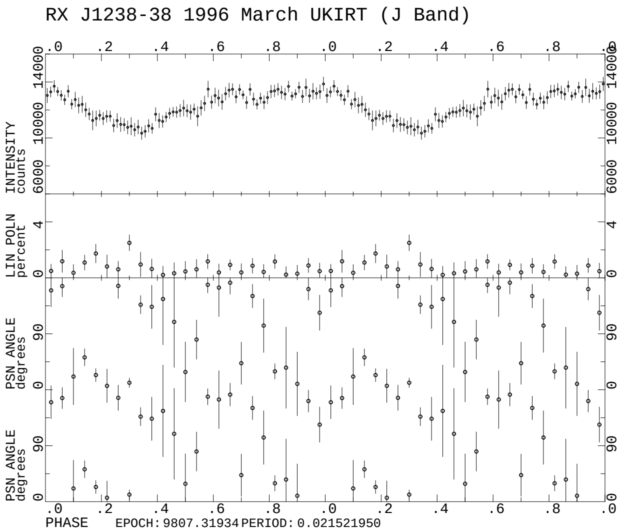

Figure 9. Phased-binned *J*-band intensity, linear polarization and position angle variations on the 1860 s period.

4.2 J-band photometry

We analysed the *J*-band intensity variations to compare the frequency spectra with those in the optical. As for the optical data, we fitted a linear trend to the dataset as a whole and used it to normalise the data: the DFT therefore produces fractional amplitude. Fig. 8 (top) shows the resulting frequency spectrum from 0 to 1 mHz. The most prominent peak is at 1949 sec. However the breadth of the window pattern permits the selection of the one and two cycle/day aliases from this central peak and the 1860 s peak (two cycles/day alias) corresponds to the most prominent peak in the optical photometry. The 1860 sec peak can therefore safely be identified as the true periodicity.

In order to establish whether there is any evidence of the 2147 s period, or any of the longer periods seen in the spectroscopy (Section 6), we have prewhitened the *J*-band data by the best fit sinusoid to the 1860 sec period (at 1863.4 sec in these data) and plotted the resulting amplitude spectrum (Fig. 8 bottom). There are no other obvious periodicities and in particular there is no evidence of any power at the 2147 sec period or around 90 minutes, a period we detect in the spectroscopy. There appears to be a broad peak of power at long periods with aliases at 5.45, 4.48, 3.75 and 3.25 hours, but it is not clear whether any of these are significant. No single observations spans more than ∼1.8 h, which hinders the detection of low frequencies associated with orbital modulations. Within the errors, none of the above mentioned periods coincide with the purported 3.86 h orbital period.

The amplitude of the *J*-band light curve folded on the 1860 sec period (shown in Fig. 9) has a larger semi-amplitude, ~ 0.14, than that in the optical (~ 0.07).

5 POLARIMETRIC VARIATIONS

The optical photopolarimety data, obtained in 1996 February and March, were initially analysed for the presence of periodic variations in the intensities. For the February data, taken using a broad red OG570 filter, the intensity variations were virtually identical to the simultaneous white-light high-speed photometry light curves. The periodogram for the March intensities was also similar to the February (and 1995) results, with the two period peaks present at 2147 s and 1860 s, and with amplitudes similar to previous photometric runs (at ∼10% and 8% respectively). One unusual dissimilarity is the presence of a strong low frequency component, at ∼0.1 mHz (∼9400 s), as seen in Fig. 6 (4th graph from the top). Although the observations were obtained in photometric conditions, in good seeing, it is not altogether impossible that this is a result of some instrumental effect, for example light loss from the aperture due to mis-centring of the star. However, this is usually noticeable as an increase in the coefficients of the low order Fourier components in the on-line results. The fact that no systematic increase was observed argues in favour of these variations being intrinsic to the star.

We then analysed the polarizations from both the SAAO and UKIRT data. The data were first transformed into Stokes parameters Q, U and V because these are linear and thus more readily interpreted. Each of the Stokes parameters in the SAAO white light and OG570 data and the UKIRT *J*-band data were Fourier analysed separately, and then all together. In each case, the mean was subtracted from the dataset as a whole, but without normalisation, so that the amplitudes calculated from the DFTs can be read off the axis directly. No significant variations are seen in any of the datasets, and in particular none at either of the photometric periods in Table 2. The results of the full dataset (recalling that UKIRT contributes only linear data) are in Fig. 10. Upper limits for any significant variations are ~ 0.4 per cent. As a last resort to search for low amplitude signals common to all of Q, U and V, and since they are independent, we have calculated their product, which is shown in the bottom panel of Fig. 10. Even this shows no evidence of periodicities at the 1860s or 2147s periods.

In Fig. 9 we show the 4 nights of *J*-band polarime-

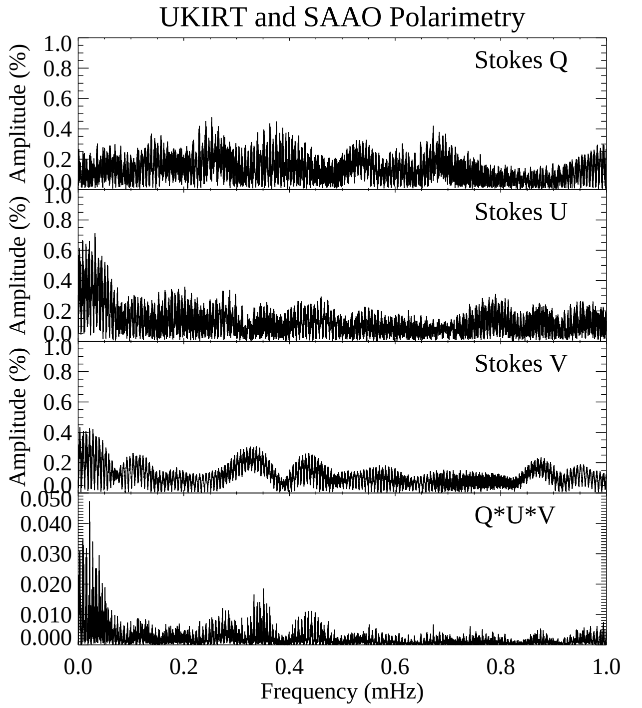

Figure 10. DFT amplitude spectra for the combined optical and IR Stokes Q, U and V parameters, plus their product.

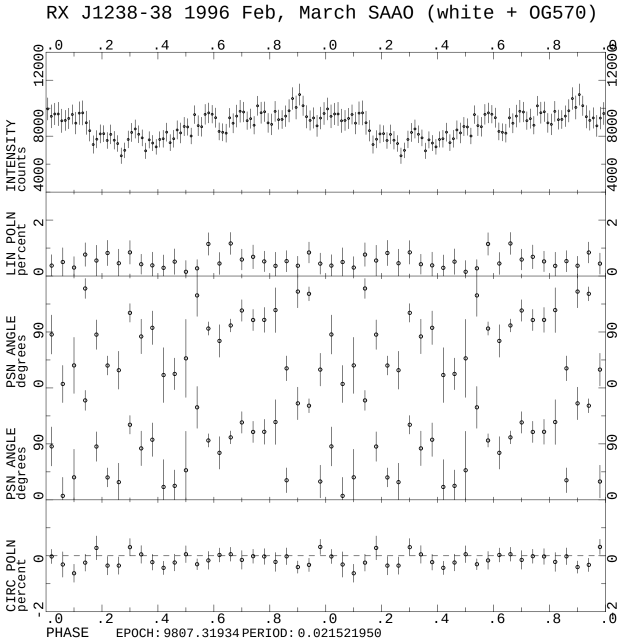

Figure 11. Optical ("white-light" and "red") intensity (top), linear polarization, position angle and circular polarization (bottom) variations, after phase binning on the 1860 s photometric period.

try phased on the 1860 s period in Table 2. The J intensity variation is slightly flat-topped. As expected from the DFTs, there is no significant linear polarization variation, but there is some evidence that there may be a systematic position angle variation of 360 degrees per spin period. This is also marginally evident in the folded (but not phase-binned) data. However, the systematic effects in the instrument and reduction procedure at this level are unquantified. Fig. 11 shows the white-light and OG570 SAAO dataset phased on the same period. The intensity variation is similar to that in the J-band (larger error bars simply reflect the different intensity levels in the two filters). None of the polarisations are significant. A coherent position angle variation is a particularly sensitive test of linear polarisation and there is some correspondence between the SAAO and UKIRT position angles. A plot of the combined datasets shows some evidence of such a coherent variation, but its appearance is dependent on the phase binning used, so we conclude that any real variation is, at most, marginal.

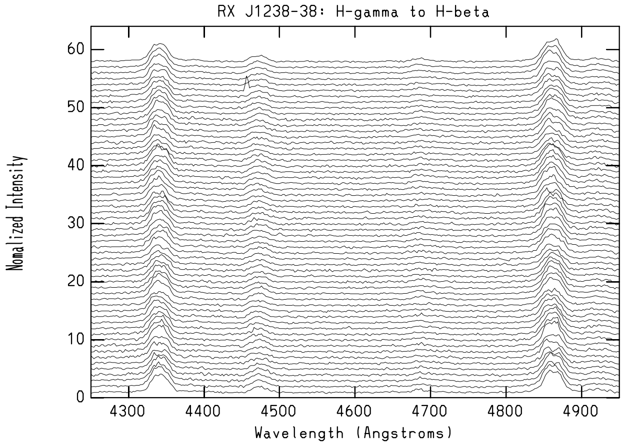

Figure 12. Continuum normalized spectra, stacked vertically in time, in the region Hγ to Hβ.

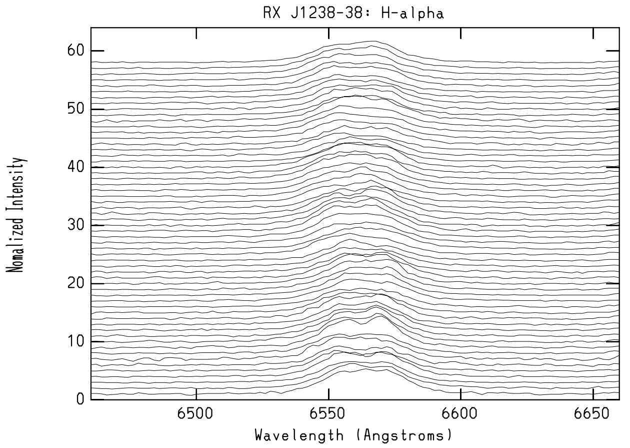

Figure 13. Same as Fig. 12, but for Hα.

6 EMISSION LINE VARIATIONS

The lines are clearly multi-component in nature, often exhibiting weak double-peaks, and a very broad base component with wings extending many 1000's km s^{-1}. In Figs. 12 and 13 we show the individual spectra, normalized to the continuum, for the Hγ, Hβ and Hα lines. Sometimes the lines show clear double components, although mostly they

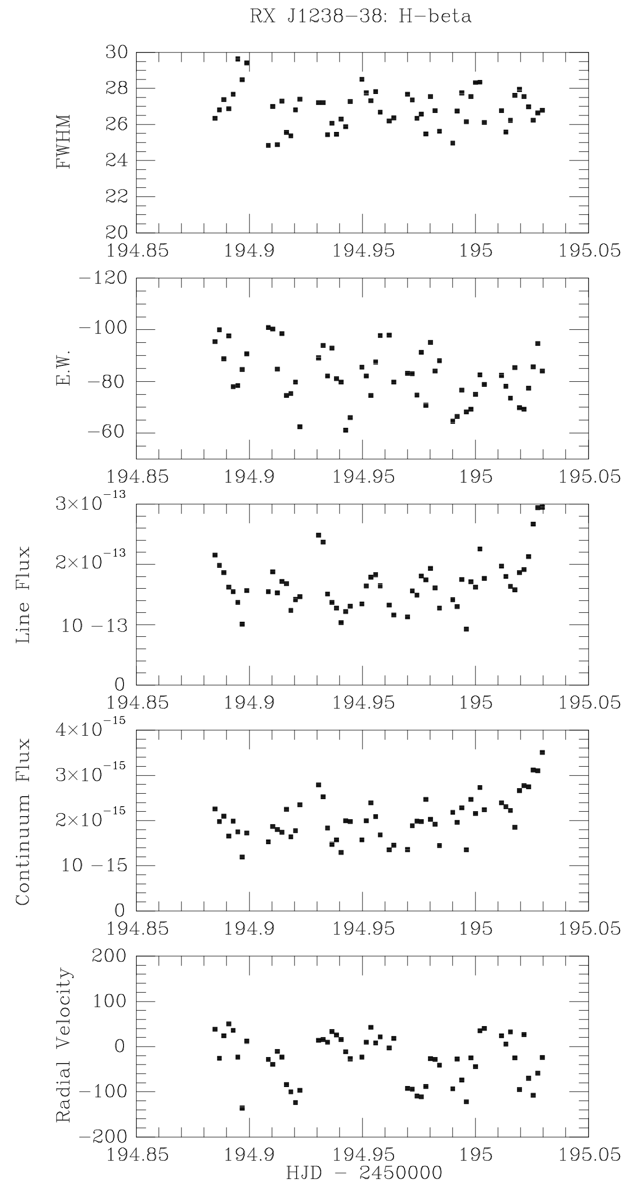

Figure 14. Line parameters for Hβ. From top to bottom: FWHM (Å), E.W. (Å), line flux (ergs cm^{-2} s^{-1}), continuum flux (ergs cm^{-2} $s^{-1}Å^{-1}$) and radial velocity (km s^{-1}).

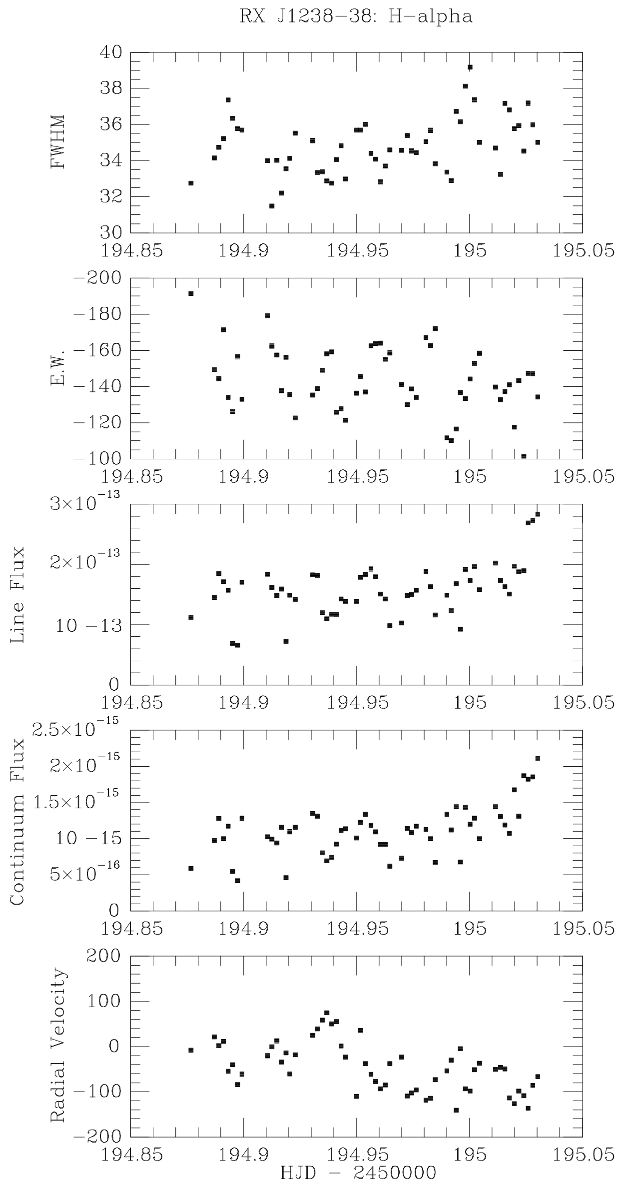

Figure 15. Line parameters for Hα. From top to bottom: FWHM (Å), E.W. (Å), line flux (ergs cm^{-2} s^{-1}), continuum flux (ergs cm^{-2} $s^{-1}Å^{-1}$) and radial velocity (km s^{-1}).

appear as broad single peaks, sometimes flattened or mildly asymmetric.

Our attempts at multiple Gaussian deblending of the Balmer lines resulted in somewhat ambiguous results. This was no doubt due to problems with contamination of line wings by other lines (e.g. HeI), and the uniqueness problem of fitting several Gaussians to broadened and blended lines.

We therefore used a single Gaussian fitting procedure to determine emission line parameters (line fluxes, widths (FWHM), eqivalent widths, radial velocities) for the 58 spectra spanning the ∼3.5 h observation. The fits are dominated by the strong line cores, rather than the broader component.

In Figs. 14 and 15 we display plots of these parameters for the Hβ and Hα lines. We subjected these data to a DFT period search, and in Fig. 16 and 17 we show the resultant periodograms. The dominant power in the line variations occurs at ∼2100 s for both Hα and Hβ, coincident, within the uncertainties, with the longer 2147 s photometric period. The emission line fluxes are clearly modulated at the 2147 s period (Fig. 18), and the E.W. variations are therefore not simply due to the continuum variability at this period. Indeed the three quantites, E.W., continuum and line fluxes, all vary in phase, implying that the emission line flux is more strongly modulated than the continuum flux.

Results for the radial velocities are more complicated, as seen in the relevant amplitude spectra (top panels in Fig. 16 and 17). Both lines exhibit a variation at the 2147 s period, and also at lower frequencies. For Hβ this lower frequency corresponds to a period of ∼5200 s (∼90 min; which is also seen as the second strongest peak for Hα), with the strongest peak for Hα corresponding to a period of 4.8 ± 1.6 h. While this latter period is coincident with the hypothesised 3.86

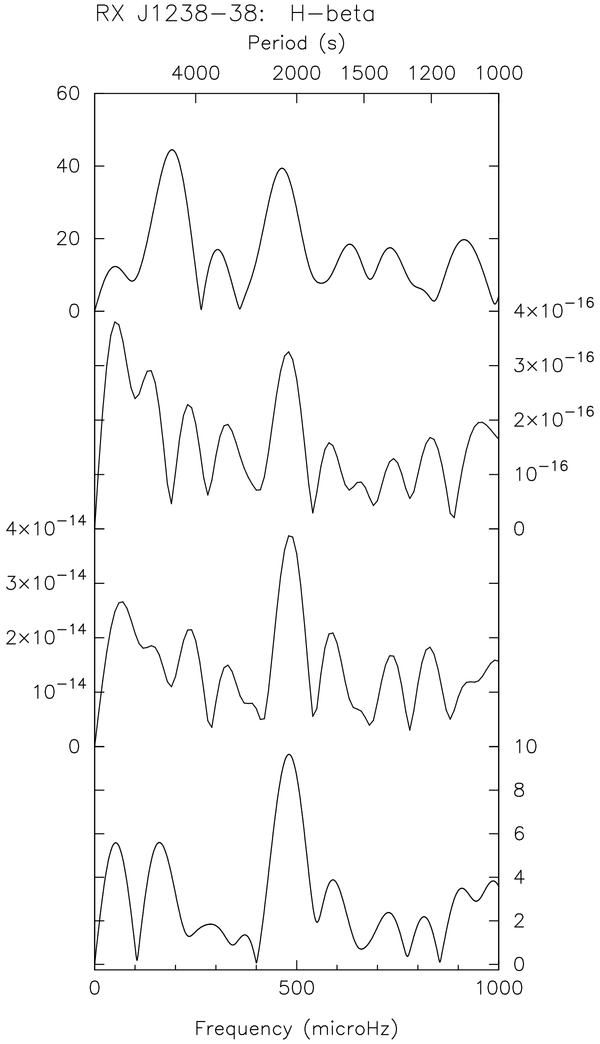

Figure 16. DFT amplitude spectra of Hβ line parameter variations. Top to bottom: radial velocity (km s^{-1}), continuum flux (ergs cm^{-2} s^{-1}Å^{-1}), line flux (ergs cm^{-2} s^{-1}) and equivalent width (Å).

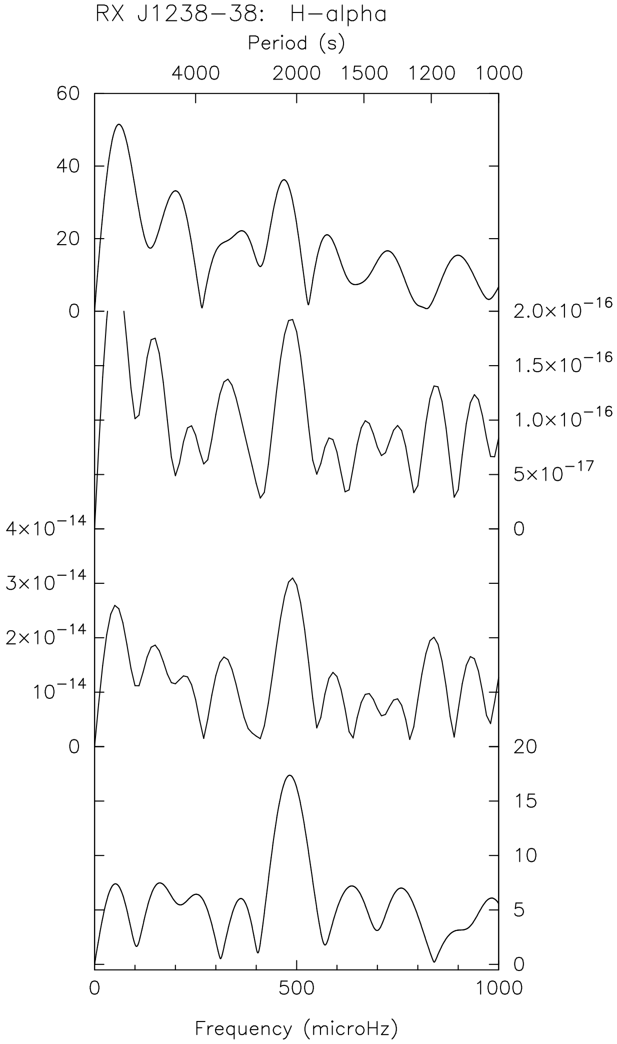

Figure 17. Same as Fig. 14, but for Hα.

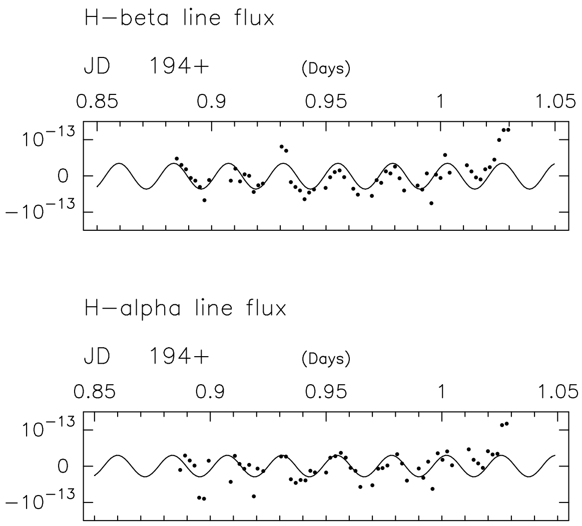

Figure 18. Hβ (upper panel) and Hα (lower panel) line flux variations (in ergs cm^{-2} s^{-1} from the mean value), plus the best-fit sinusoids at 2147 s.

h orbital period, it should be noted that the data hardly adequately samples this period.

We completed the radial velocity analysis by using a cross-correlation technique on all the emission lines in the spectral region 3700−5100Å. This potentially produces a more reliable radial velocity curve, which utilises information from all of the emission lines simultaneously. First the spectra were rebinned to logλ, and a template spectrum formed from the grand sum. Spectra were then flattened by normalization of the continuum, defined by a spline fit to line-free regions of the spectrum. The results were similar to those for Hβ, and the power spectrum of the radial velocities was very similar, with two peaks at $\sim$5200 and $\sim$2100 s. We show these cross-correlation velocities, plus the best fit of the two sinusoids at these frequencies, in Fig. 19 (top panel).

If we accept these radial velocity results at face value, then we are forced to conclude that the longer period is in fact the orbital period, and that 2147 s is the spin period. This contradicts the earlier hypothesis, based on the supposed identification of the 1860 s and 2147 s photometric periods as the spin (ω) and synodic ($\omega - \Omega$) frequencies.

However, we believe that the radial velocities are a more reliable indicator of both orbital and spin period. In all other IPs, it is precisely these periods which dominate the radial velocity variations. The one apparent exception is the system RX J1712.6−2414 (Buckley et al. 1995, 1997), which has been convincingly shown to be a discless IP, seen nearly pole-on. In this system there is no detectable orbital radial velocity (Sekiguchi & Buckley 1995), while the synodic ($\omega - \Omega$) frequency, rather than the spin (ω) frequency, is seen in the radial velocities. Further discussion of this point, in relation to possible interpretation of the RX J1238–38 results, is left until later.

Finally we comment on the relative phasing of the short period (~2100 s) radial velocity and line width (FWHM) variations. The line widths and radial velocities appear to be anti-phased, with maximum line width occuring at maximum blue-shift of the lines (Fig. 19). If the lines are produced in a curtain of material accreting onto both magnetic poles (e.g. Hellier et al. 1987; Rosen, Mason & Córdova 1988; Hellier, Cropper & Mason 1991), then we can interpret our observations in the following way. The upper, partially optically thick (in the emission lines), accretion curtain contributes most of the line flux, the lower curtain being partially obscured by the accretion disc. When it is closest to the observer, the upper curtain more successfully obscures both the white dwarf, the lower accretion curtain and the narrowing 'neck' of the accretion funnel. The observer therefore sees mostly gas from the back of the curtain, where it is lifted out of the disc plane. For modest inclination angles ($i \gtrsim 45°$), the gas is mostly moving transversely to the line of sight, or with a predominantly recessional component (i.e. red-shifted). Half a spin cycle later, we view the other side of the curtain, including the higher velocity gas in the narrowing funnel, which is mostly blue-shifted. Since we see a larger range of, and higher, velocities, we expect that the resulting Doppler broadening will be at maximum. That we may also glimpse part of the lower curtain at this phase only increases the effect. The net result is that the γ-velocity should be negative, and the emission line widths and radial velocities anti-phased, with maximum blue-shift of the lines coinciding when they are also widest. This is precisely what is observed in RX J1238–38, where the FWHM varies from ~1400 to 1900 km s^{-1}.

7 IDENTIFYING THE ORBITAL AND SPIN PERIODS

The results from the photometry and spectroscopy appear, at face value, to be contradictory. Taking the photometric results on their own, we conclude that RX J1238–38 is an IP exhibiting almost equal amplitude spin and synodic (beat) periods. If we make the conventional interpretation that the longer period (2147 s) is the first orbital sideband (synodic) period, and the shorter one (1860 s) the spin period, then we conclude that the orbital period is ~3.86 h, a value quite typical of IPs with spin periods in the range 1000−2000 s (Warner 1995).

However, this picture appears not to be confirmed from the emission line analysis. We found that the emission line

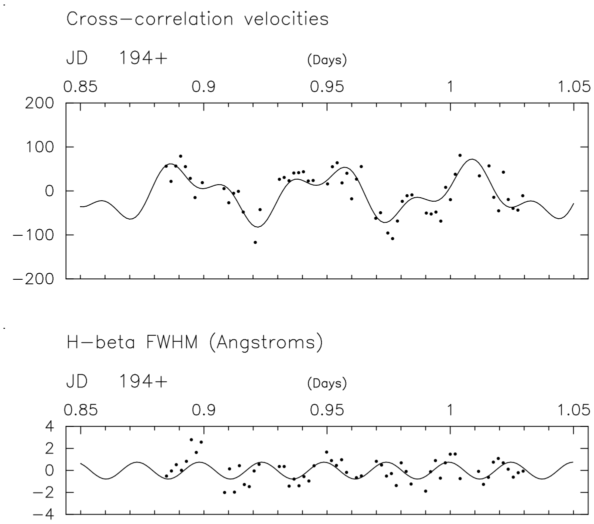

Figure 19. Cross-correlation emission line radial velocities (km s^{-1} ; top) and Hβ line widths (variation of FWHM from the mean, in Å; bottom), plus the best-fitting sinusoids of the spectroscopic periods 2147 s and 5700 s, for the radial velocities, and the 2147 s period only, for the line widths.

fluxes, widths and radial velocities were all dominantly modulated at the *longer* period of 2147 s. In all but one extreme case, emission lines in IPs vary at the spin period, rather than the synodic period. This would suggest that the 2147 s period is indeed the spin period of the system. The exception is RX J1712.6−2414, which is the strongest polarized IP known to date (Buckley et al. 1995). In this case it appears that the magnetic field is strong enough to prevent an accretion disc from forming (Buckley et al. 1997), and that the bulk of the accretion is "discless", in that the accretion stream from the secondary star penetrates directly into the white dwarf's magnetosphere. For this reason, the photometric, X-ray and radial velocity periods are all at the *synodic* value (Buckley et al. 1997), with only the circular polarization being modulated at the shorter spin period. Even in the case of the radial velocities, the lines are only weakly modulated at the synodic period, with a very small amplitude (probably due to the extreme low inclination). We have no reason to believe that the emission lines variations in RX J1238–38 occur at the synodic period. Our search for circular polarization in RX J1238–38 gave an inconclusive result, ruling out any similarity with RX J1712.6−2414 in this regard. We therefore conclude that the weight of evidence favours 2147 s as the spin period of RX J1238–38.

What about the orbital period of RX J1238–38? We have seen that there was little observational evidence supporting the hypothesis that the orbital period is 3.86 h. Radial velocities are a far more reliable indicator of the orbital period than photometric variability. We found from the analysis of the emission lines that the dominant radial velocity period was at 5300 $^{+1260}_{-850}$ s (~88 $^{+21}_{-14}$ m), although from the small stretch (3.5 h) of single-night data, the period is rather imprecise. We therefore adopt this as being the most likely orbital period of the system, making it the lowest orbital period IP (in fact near the minimum period for CVs), and only the second system, together with EX Hya, below the period gap. Indeed it is perhaps worth mentioning at this point that the spectrum of RX J1238–38, and the emission lines in particular, are very similar to EX Hya. Both systems have the most extreme values for emission line widths in IPs, with EX Hya having FWZI ∼7000 km s^{-1} (Hellier et al. 1987) and RX J1238–38 ∼6000 km s^{-1}.

If the above picture is correct, namely that the spin period is 2147 s, we now ask what produces the other photometric period, at 1860 s ? It clearly cannot be any of the fundamental orbital sideband frequencies ($\omega + \Omega, \omega + 2\Omega$), since they are all too far away from the observed peak. Also, it is not expected that the positive sidebands could dominate over the usually more powerful negative sidebands (e.g. Warner 1986). The only remaining possibilities are harmonics of the sidebands. One which is close enough to consider is the harmonic at $\nu = 2(\omega - \Omega)$, whose predicted value is $1804\ ^{+270}_{-210}$ s. If we assume that the 1860 s period is indeed this harmonic, then we can refine our estimate of the orbital period from $(\Omega)^{-1} = (\omega - \nu/2)^{-1} = 5077$ s $= 84$ min, which is within the uncertainties estimated for P_{orb} above.

8 DISCUSSION

We have presented conclusive observational evidence that RX J1238–38 is new member of the Intermediate Polar class of magnetic CVs. Furthermore, the weight of evidence favours a 2147 s (36 min) spin period and an 84 min orbital period. However, an alternative, less well supported hypothesis, has the spin period identified as 1860 s period, and the other photometric period, at 2147 s, as the first orbital sideband frequency (i.e. the synodic period), implying a 3.86 h orbital period.

If the former interpretation is correct, then RX J1238–38 becomes only the second IP below the 2−3 h "period gap". In many respects RX J1238–38 resembles the only previously known below-gap system, EX Hya. In this model, the best explanation for the other photometric period, at 1860 s (31 min), is that it is most likely the harmonic of the synodic period. Its large amplitude relative to the spin period makes it unusual amongst IPs, where usually one or other period dominates. Initial explanations for synodic variations in IPs usually involved reprocessing of X-rays off the disc hot-spot and/or the secondary star (e.g. Wickramasinghe, Stobie & Bessell 1982; Buckley & Tuohy 1988). Recently it has been suggested that direct stream fed accretion plays a more important role, where a component of the accretion stream overshoots the disc, impinging directly into the magnetosphere (Hellier 1993; Hellier & Livio 1994; Buckley 1997). We note that TX Col, an IP for which this mode of accretion has recently been invoked (Norton et al. 1997), has at least on one occasion shown the harmonic of the synodic frequency, $2(\omega - \Omega)$, dominating the optical power spectrum (Buckley & Sullivan 1992). Such a dominance of the first harmonic, over the fundamental, can be explained in terms of two-pole accretion. Hence the 1860 s period could be a result of direct accretion onto *both* the magnetic poles, plus a component due to reprocessed radiation.

RX J1238–38 also shows a marked increase in the amplitude of the 1860 s period at longer wavelengths: ∼14% in J compared to ∼7% "white-light". Also the I-band light curve shows a comparitively higher pulse amplitude than the B-band. This behaviour contrasts with FO Aqr, the only IP for which amplitudes have been well determined from the optical to IR (de Martino et al. 1994). Here the synodic $(\omega - \Omega)$ amplitudes were ∼5% and 6%, respectively, for J and B. de Martino et al. (1994) found that the synodic pulse spectrum had a characteristic temperature of 7300K, and concluded that it was most likely a result of X-ray reprocessing. The larger amplitude in the IR for RX J1238–38, if interpreted as reprocessing from both poles, could be a result of either a cooler temperature or that the reprocessed radiation is a relatively more important contributor to the overall IR flux. In contrast the 2147 s spin pulse appears to have a stronger amplitude at *shorter* wavelengths, judging from the B *and* I light curves. This result is typical of IPs, where the spin modulated spectrum is a hot source, for example 11300K in FO Aqr (de Martino et al. 1994).

In terms of the alternative model, where the spin period is 1860 s, the larger IR modulation may be a result of cyclotron emission. The fact that both the optical ("white-light") and IR (J-band) light curves, binned at 1860 s, have in-phase maxima (compare Figs. 7b and 9) are also explained in the accretion curtain model. Both the optical and IR (cyclotron) radiation escapes more readily from the sides of the curtain, due to decreased optical depth in that direction and cyclotron beaming.

Although there is scant X-ray data at present on RX J1238–38, it is interesting to speculate whether this two-pole accretion will be observed in X-rays. For EX Hya, which we have already shown exhibits similarities to RX J1238–38, Rosen et al. (1991) reported that their GINGA observations supported a model with two emission regions, above and below the orbital plane.

The very strong and broad Balmer emission lines are also very reminiscent of EX Hya, and are modulated in strength and width at the spin period. The line intensity amplitude actually exceeds that of the continuum, while the width is anti-correlated with the radial velocities. This can be qualitatively understood in terms of varying viewing aspect of the accretion curtains.

Finally we note that the purported ∼84 min orbital period, which we prefer to the alternative 3.86 h period, is very close to the lower orbital period limit for CVs in which the secondary remains non-degenerate. Like EX Hya, RX J1238–38, which is even more closely synchronous, could have a non-equilibrium spin period as a result of long term deviations of the mass transfer rate from the secondary star.

According to the diamagnetic accretion model of Wynn and King (1998, in preparation) the spin period of the white dwarf in IPs below the period gap is restricted by the corotation radius approaching the limit set by the distance to the L1 point. Their model implies that the ratio of spin to orbital periods should be ∼ 0.5, and they have noted that for EX Hya the ratio is 0.7 and for RX J1238–38 the ratio is 0.42. Their model is therefore compatible with this second system below the period gap. (See also Wynn, King & Horne 1997, MNRAS, 286, 436.)

ACKNOWLEDGEMENTS

We thank the SAAO and UKIRT staff for their technical support. DAHB thanks M. Mouchet for bringing RX J1238–38 to his attention, and to M. Pierre for the providing further information. We gratefully acknowledge Darragh O'Donoghue, for the use of his period analysis software, EAGLE. Part of this work was undertaken when one of us (DAHB) was a Visiting Fellow at the Australian National University's Astrophysical Theory Centre.

We are also grateful to the referee, Dr Mike Watson, and to Dr Graham Wynn for some useful comments.

REFERENCES

Buckley D.A.H., 1997, in Wickramasinghe D.T., Bicknell G.V., Ferrario, L., eds, ASP Conf. Ser., Vol. 121, Accretion Phenomena and Related Outflows. Astron. Soc. Pac., San Franciso, p.420

Buckley D.A.H., Tuohy I.R., 1988, ApJ, 344, 376

Buckley D.A.H., Sullivan D.J., 1992, in Vogt N.,ed, ASP Conf. Ser., Vol. 29, Vina del Mar Workshop on Cataclysmic Variable Stars. Astron. Soc. Pac., San Francisco, p. 387.

Buckley D.A.H., Sekiguchi K., Motch C., O'Donoghue D., Chen A.-L., Schwarzenberg-Czerny A., Pietsch W., Harrop-Allin M., 1995, MNRAS, 275, 1028

Buckley D.A.H. Haberl F., Motch C., Pollard K., Schwarzenberg-Czerny A., Sekiguchi K., 1997, MNRAS, in press

Cropper M., 1985, MNRAS, 212, 709

de Martino D., Buckley D.A.H., Mouchet M., Mukai M., 1994, A&A, 285, 125

Deeming, T.J., 1975, Astrophys. Space Sci., 36, 137

Haberl F. & Motch, C., 1995, A&A, 297, L37

Haberl F., Thorstensen J.R., Motch C., Scwarzenberg-Czerny A., Pakull M., Shambrook A., Pietsch W., 1994, A&A, 291, 171

Hellier C., 1993, MNRAS, 265, L35

Hellier C., Cropper M.S., Mason K.O., 1991, MNRAS, 248, 333

Hellier C, Livio M., 1994, ApJ, 424, L57

Hellier C., Mason K.O., Rosen S.R., Córdova F., 1987, MNRAS, 242, 32P

Kurtz, D.W., 1985, MNRAS, 213, 773

Mason K.O. et al., 1992, MNRAS, 258, 749

Mateo M., Schechter P.L., 1989, in Grösbol P.J., Murtagh F., Warmaels R. H., eds, ESO Conf. Workshop Proc. No. 31, 1st ESO/ST-ECF Data Analysis Workshop, ESO, Garching, p.69

Motch C., Haberl F., 1995, in Buckley D.A.H., Warner B., eds, ASP Conf. Ser., Vol. 85, Cape Workshop on Magnetic Cataclysmic Variables. Astron. Soc. Pac., San Franciso, p.109

Motch C., Haberl F., Guillout P., Pakull M., Reinsch K., Krautter J., 1996, A&A, 307, 459

Norton A.J., Hellier C., Beardmore A.P., Wheatley P.J., Osborne J.P., Taylor P., 1997, MNRAS, 289, 362

Rosen S.R., Mason K.O, Córdova F., 1988, MNRAS, 231, 549

Rosen S.R., Mason K.O., Mukai K., Williams O.R., 1991, MNRAS, 249, 417

Sekiguchi K., Buckley D.A.H., 1995, in Buckley D.A.H., Warner B., eds, ASP Conf. Ser., Vol. 85, Cape Workshop on Magnetic Cataclysmic Variables. Astron. Soc. Pac., San Franciso, p.281

Serkowski K., 1974, in Gerhels T., Planets, Stars and Nebulae Studied with Photopolarimetry. University of Arizona, Tucson, p. 135

Szkody P., 1995, in Buckley D.A.H., Warner B., eds, ASP Conf. Ser., Vol. 85, Cape Workshop on Magnetic Cataclysmic Variables. Astron. Soc. Pac., San Franciso, p.54

van der Woerd H., de Kool M., van Paradijs J., 1984, A&A, 131, 137

Verbunt F., Bunk W. H., Ritter H., Pfeffermann E., 1997, A&A, in press.

Voges, W., et al, 1997, in press, A&A

Warner, B., 1986, MNRAS, 219, 347

Warner B., 1995, Cataclysmic Variable Stars. Cambridge University Press, Cambridge, p.367

Warner, B., O'Donoghue D., Fairall, A.P., 1981, MNRAS, 196, 705

Whittet D. C. B., Martin P. G., Hough J. H., Rouse M. F., Bailey J. A., Axon D. J., 1992, ApJ, 386, 562

Wickramasinghe D.T., Stobie R.S, Bessell, M.S., 1982, MNRAS, 200, 605

Wynn G., King A.R., Horne K., 1997, MNRAS, 286, 436.